Weak Coupling of ATP Hydrolysis to the Chemical Equilibrium of Human Nicotinamide Phosphoribosyltransferase†

Emmanuel S. Burgos and Vern L. Schramm*

Department of Biochemistry, Albert Einstein College of Medicine, 1300 Morris Park Avenue, Bronx, New York 10461

Received June 26, 2008; Revised Manuscript Received August 7, 2008

ABSTRACT: Human nicotinamide phosphoribosyltransferase (NAMPT, EC 2.4.2.12) catalyzes the reversible synthesis of nicotinamide mononucleotide (NMN) and inorganic pyrophosphate (PP_i) from nicotinamide (NAM) and α-D-5-phosphoribosyl-1-pyrophosphate (PRPP). NAMPT, by capturing the energy provided by its facultative ATPase activity, allows the production of NMN at product:substrate ratios thermodynamically forbidden in the absence of ATP. With ATP hydrolysis coupled to NMN synthesis, the catalytic efficiency of the system is improved 1100-fold, substrate affinity dramatically increases (K_m^{NAM} from 855 to 5 nM), and the K_{eq} shifts −2.1 kcal/mol toward NMN formation. ADP−ATP isotopic exchange experiments support the formation of a high-energy phosphorylated intermediate (phospho-H247) as the mechanism for altered catalytic efficiency during ATP hydrolysis. NAMPT captures only a small portion of the energy generated by ATP hydrolysis to shift the dynamic chemical equilibrium. Although the weak energetic coupling of ATP hydrolysis appears to be a nonoptimized enzymatic function, closer analysis of this remarkable protein reveals an enzyme designed to capture NAM with high efficiency at the expense of ATP hydrolysis. NMN is a rate-limiting precursor for recycling to the essential regulatory cofactor, nicotinamide adenine dinucleotide (NAD^+). NMN synthesis by NAMPT is powerfully inhibited by both NAD^+ ($K_i = 0.14$ μM) and NADH ($K_i = 0.22$ μM), an apparent regulatory feedback mechanism.

The properties of NAD^+ [1] in electron transfer are now established. As a cofactor in many metabolic pathways, NAD^+ holds a key position in energy metabolism and its regulation. Over the past decade, new facets of involvement for NAD^+ were discovered. It is used by poly- and mono(ADP-ribose) polymerases as a substrate for protein covalent modifications (*1*−*5*).

Sirtuins (SIRT) use NAD^+ in protein deacetylation reactions which has implications for metabolic control, cancer, and longevity. While redox reactions do not influence the net level of NAD^+ and NADH concentrations, enzymes that catalyze ADP ribosylation and deacetylation cleave the N-ribosyl bond to nicotinamide and can lead to a rapid depletion of this substrate. NAD^+ levels influence all of its associated pathways, and the NAD^+ pool needs constant replenishment from NAM recycling since dietary sources of the vitamin may be limiting.

In prokaryotes and lower eukaryotes, NAD^+ replenishment is achieved primarily by de novo synthesis. Quinolinic acid, derived from tryptophan, is converted into nicotinic acid mononucleotide (NAMN) by the quinolinic acid phosphoribosyltransferase (QAPT). NAMN, obtained from exogenous nicotinic acid (NA) by reaction with nicotinic acid phosphoribosyltransferase (NAPT), is converted into NAD^+, via the Preiss−Handler pathway (*6*). The salvage pathway for those organisms (*4, 7*) involves the deamination of NAM into NA via the corresponding nicotinamidase (Pnc1). Mammals lack Pnc1 and directly convert NAM into nicotinamide mononucleotide (NMN) with nicotinamide phosphoribosyltransferase (NAMPT). NMN is converted to NAD^+ by nicotinamide/nicotinic acid mononucleotide adenylyltransferase (NMNAT) (Scheme 1).

NAD^+ is not localized uniformly in the cell, with up to 70% of the pool held in the mitochondria (*8*). Three isoforms of NMNAT are known, and each has a specific subcellular localization (*9*−*13*). NMNAT-3 is located mainly in the mitochondria, and mitochondrial NAD^+ is proposed to influence cell lifespan, together with the overexpresssion of SIRT enzymes (*14, 15*). In yeast, overexpression of NAPT, NMNAT, and Pnc1 increased the activity of NAD^+-dependent histone deacetylase (Sir2) (*16*−*18*). In mammals, NAMPT is the rate-limiting enzyme for salvage of NAD^+ from NAM, and its overexpression lengthened the cell lifespan (*19*). This phenomenon is apparently associated with the increased catalytic activity of the mammalian ortholog of Sir2, SIRT1 (*20*). Recently, NAMPT was identified as the enzyme regulating mitochondrial NAD^+ levels (*21*) and increasing

† This work was supported by Grant GM41916 from the National Institutes of Health.

* To whom correspondence should be addressed: Department of Biochemistry, Albert Einstein College of Medicine, 1300 Morris Park Ave., Bronx, NY 10461. Telephone: (718) 430-2813. Fax: (718) 430-8565. E-mail: vern@aecom.yu.edu.

[1] Abbreviations: NAMPT, nicotinamide phosphoribosyltransferase; NMN, nicotinamide mononucleotide; PP_i, pyrophosphate; PCP, methylenediphosphate; PNP, imidodiphosphate; NAM, nicotinamide; PRPP, α-D-5-phosphoribosyl-1-pyrophosphate; NAD^+, nicotinamide adenine dinucleotide; SIRT, sirtuins; NAPT, nicotinic acid phosphoribosyltransferase; NAMN, nicotinic acid mononucleotide; NA, nicotinic acid; QAPT, quinolinic acid phosphoribosyltransferase; NMNAT, nicotinamide/nicotinic acid mononucleotide adenylyltransferase; FK866, (*E*)-*N*-[4-(1-benzoylpiperidin-4-yl)butyl]-3-(pyridin-3-yl)acrylamide; THP, tris(hydroxypropyl)phosphine; Ap5A, P^1,P^5-di(adenosine-5′-)pentaphosphate; mS, millisiemens.

10.1021/bi801198m CCC: $40.75
Published on Web 09/30/2008

Scheme 1: Reaction Catalyzed by Human NAMPT and Inhibitors

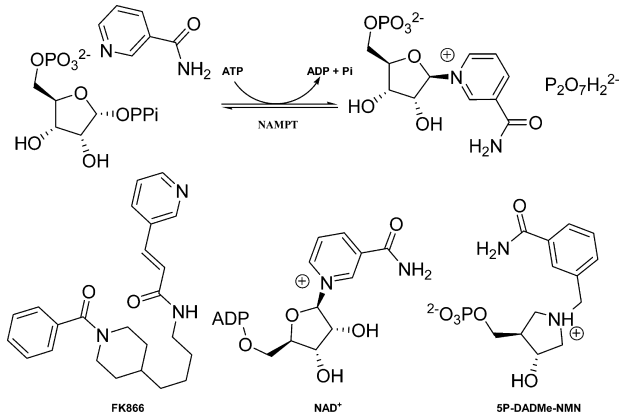

cell lifespan via sirtuins, SIR3 and SIR4, both located in this organelle.

The crucial role of NAMPT in NAD^+ biosynthesis makes it an attractive target in regulation of mammalian metabolic and regulatory pathways. Modulation of NAMPT activity through inhibition or activation could lead to a shorter or extended lifespan, respectively. Inhibition of NAD^+ salvage by specific inhibition of NAMPT has been described previously (*22*). The small molecule inhibitor, FK866, decreased the size of the NAD^+ pool via inhibition of this enzyme (K_i = 0.4 nM). Reducing the activity of NAMPT by FK866 in human vascular smooth muscular cells caused low levels of NAD^+ and caused a decrease in SIRT1 activity (*20*). Under these conditions, SIRT1 failed to deacetylate tumor suppressor p53 and this transcription factor was kept at levels above those which induce cell senescence.

FK866 is in clinical trials, but it exhibits low bioavailability, rapid intravenous clearance, and substantial drug binding to plasma proteins (*23*). Continuous intravenous infusions over 96 h for a period of 4 weeks showed no objective responses. Finally, inhibition by FK866 was reversible upon NAM injection. Isosteric analogues of the inhibitor have been synthesized without improved inhibition properties against NAMPT (*24*).

Structural analyses of mammalian NAMPTs have provided a guide to substrate−protein and inhibitor−protein interactions (*25*−*27*). Catalytic site contacts together with mechanisms from related phosphoribosyltransferases have been used to propose a molecular mechanism for NAMPT. However, human NAMPT displays weak sequence identity with other members of this family, although *Thermoplasma acidophilum* dimeric NAPT has been proposed as a structural homologue (*28*). The kinetic mechanism of *Salmonella typhimurium* NAPT is the most complete and is useful in analysis of NAMPT (*29*). This NAPT also couples ATP hydrolysis and NAMN synthesis, to shift the dynamic equilibrium toward NAMN. Its ATPase activity involves a phosphohistidine intermediate (*30*−*32*), and most rate constants fot the mechanism have been established (*33, 34*). NAMPT is also similar to NAPT as its catalytic efficiency is improved by ATP (*35*).

Unlike NAPT, the catalytic features and reaction mechanism of human NAMPT are poorly described. Crystallographic structures are useful for proposing catalytic residues but offer few insights into the energetic and kinetic mechanisms. Likewise, the covalent phospho-NAMPT structure had not been revealed in the reported structures, and no thermodynamic properties have been reported.

Here we describe the role of ATP in NMN synthesis catalyzed by NAMPT. The thermodynamic and kinetic properties of NAMPT demonstrate weak coupling of ATP hydrolysis to the dynamic chemical equilibrium and to the kinetic properties essential for nicotinamide salvage. The existence of a covalently phosphorylated enzyme involved in the mechanism is strongly supported by isotope exchange experiments and formation of a readily hydrolyzable intermediate in the presence of ATP. The kinetic mechanism defined here provides unique insights into cellular NAD^+ recycling and defines essential information required for the kinetic and thermodynamic analysis of this critical enzyme.

EXPERIMENTAL PROCEDURES

Materials. [$CONH_2$-^{14}C]NAM (55 mCi $mmol^{-1}$) was from American Radiolabeled Chemicals. [4-^{3}H]NMN (1.8 Ci $mmol^{-1}$) was from Moravek. [2,8-^{3}H]ATP and ADP (27.8 and 40 Ci $mmol^{-1}$, respectively) and [^{14}C]NAD^+ (253 mCi $mmol^{-1}$) were from Perkin-Elmer. Liquid scintillation cocktail (UltimaGold) was from Perkin-Elmer. Pyruvate kinase (PK), lactate dehydrogenase (LDH), alcohol dehydrogenase (ADH), and inorganic pyrophosphatase (PPase) were from Sigma. NMNAT-3 was overexpressed as previously described (*13*) from the corresponding plasmid (pPROEX, generous gift from H. Zang, Department of Biochemistry, University of Texas, Austin, TX). Ni-NTA resin and tris(hydroxypropyl)phosphine (THP) were from Novagen, and HiLoad Superdex 200GP 26/60 was from Amersham. HPLC solvents were from Fisher, and other biochemicals were from Sigma.

Overexpression and Purification of Human NAMPT. The enzyme was overexpressed in *Escherichia coli* BL21(DE3)-p*Lys* containing expression plasmid pBAD DEST 49 with inserts of chemically synthesized DNA (DNA 2.0) encoding human NAMPT and optimized for expression in *E. coli*. Cells were grown in LB broth containing 100 μg mL^{-1} ampicilin and 30 μg mL^{-1} chloramphenicol at 37 °C to an A_{600} of 0.4. The cultures were supplemented with 0.2% L-arabinose for induction and incubated for an additional 16 h at 37 °C preceding harvest. Resuspended cells [20 mM Tris buffer, 500 mM NaCl, 5 mM imidazole (pH 7.9), 1 mM βME, and protease inhibitor cocktail] were disrupted with a French press. Debris was removed by centrifugation at 20000 rpm for 20 min. The supernatant (150 mL from 50 g of cells) was loaded onto a Ni-NTA column (50 mL of resin preequilibrated with disruption buffer). The column was washed consecutively with buffers having imidazole concentrations of 10, 30, 50, 100, and 200 mM. The enzyme, eluted at 100 and 200 mM imidazole, was concentrated, desalted, and further purified on a HiLoad Superdex 200GP 26/60 column eluted with 100 mM HEPES (pH 7.5), 100 mM NaCl, and 10 mM βME at a flow rate of 1 mL min^{-1}. The purified enzyme (10 mg mL^{-1}) was then concentrated (50−75 mg mL^{-1}) and frozen.

Product Purification. For the isolation of radioactive [^{14}C]NMN formed from [^{14}C]NAM during kinetic experiments, [^{3}H]NAM formed from [^{3}H]NMN during equilibrium conditions, and [^{3}H]ATP formed from [^{3}H]ADP during

isotope exchange reactions, quenched samples were injected (250 μL) onto a Luna C_{18}^2 column (4.6 mm × 150 mm, 5 μm, 100 Å, Phenomenex) equilibrated in 100 mM K_2HPO_4 and 8 mM tetrabutylammonium sulfate (pH 6.0) (buffer A) and initially eluted with 4 mL of this buffer. Further elution was performed with a 16 mL linear gradient to 30% acetonitrile in the same buffer (buffer B). A flow rate of 1 mL min^{-1} was employed. NMN elutes 2.5 mL after injection, NAM at 6.2 mL, ADP at 18.7 mL, and ATP at 21.6 mL (method 1). This purification protocol does not degrade the resolution of the column if frequent acetonitrile−tetrahydrofuran−acetonitrile wash cycles are performed. To directly characterize the ATPase activity of NAMPT, quenched samples were injected (100 μL) onto a Nucleosil 4000-7 PEI strong anion exchange column (4.0 mm × 250 mm, 5 μm, 100 Å, Macherey-Nagel) equilibrated in 20 mM Tris (pH 8.2) (buffer C) and initially eluted with 5 mL of this buffer. Further elution was performed with a 30 mL linear gradient to 1 M KCl in the same buffer (buffer D). A flow rate of 1 mL min^{-1} was employed. ADP elutes 25 mL after injection and ATP at 33 mL (method 2).

Preparation and Reading of Radioactive Samples. Each radioactive sample (HPLC) was diluted with 50 mg of cold NAM prior to being freeze-dried. The resulting solid was redisolved in a 1:10 mixture (water/scintillation cocktail) prior to radioactivity determination (Wallac instrument, 20 min reading, three cycles).

Analysis of Data. All results from kinetic and inhibition studies were fit to the appropriate equations using KaleidaGraph (Synergy Software). The enzyme is described by its turnover rate and Michaelis constants, specific for each substrate involved (k_{cat} and K_m). The inverse of the initial velocity (V_A^{app}) at the corresponding inverse concentration of substrate A ([A]) follows a linear relation (Lineweaver−Burk representation) at total enzyme concentration $[E]_T$:

$$\frac{1}{V_A^{app}} = \frac{K_m^A}{k_{cat}[E]_T}\frac{1}{[A]} + \frac{1}{k_{cat}[E]_T} \quad \text{(I)}$$

For competitive inhibition studies, the inhibition constant K_i is described by the expression

$$V^I = \frac{V_{max}[A]}{K_m^A\left(1 + \frac{[I]^*}{K_i}\right) + [A]} \quad \text{(II)}$$

where V^I is the initial rate at the corresponding concentration of inhibitor [I]. For low concentrations of inhibitor (<10 times $[E]_T$), the free inhibitor concentration in solution ([I]*) and the inhibitor concentration added ([I]) are different and related by

$$[I]^* = [I] - \left(1 - \frac{V^I}{V}\right)[E]_T \quad \text{(III)}$$

where V is the initial rate of the reaction without inhibitor. K_m and K_i are also related by the following relationship:

$$K_m^{app} = K_m + \frac{K_m}{K_i^B}[B] \quad \text{(IV)}$$

Each experiment was carried out in duplicate.

Enzyme Activity−Stability Determination. To determinate the pH dependence of NAMPT activity, the enzyme (30 nM) was preincubated at 25 °C with 1 μM radiolabeled NAM (100 mM universal buffer with a constant ionic strength of 60 mS at various pH values, 1 mM ATP, 5 mM $MgCl_2$, and 1 mM THP), and the reaction was started by addition of α-D-5-phosphoribosyl-1-pyrophosphate (PRPP) (200 μM). Quenching was performed after 1 h, and samples were processed according to method 1 to monitor NMN formation. In a similar way, to determinate its stability, 10 different mixtures of enzyme (30 nM, 1 mL at various pHs) were preincubated for 1 h, then concentrated, and transferred to the previously described reaction mixture (at pH 7.6). The assay conditions were the same. The ATPase activity was evaluated by monitoring the steady-state formation of ADP. The reaction (0.75 μM enzyme, 100 mM universal buffer, 5 mM $MgCl_2$, and 1 mM THP) was initiated by addition of ATP (2 mM). Quenched samples were analyzed by HPLC (method 2).

NAMPT Autophosphorylation. Although the presumed phosphorylated NAMPT was unstable to isolation, under the conditions where the assays were performed [46 μM NAMPT, 50 mM HEPES (pH 7.5), 100 mM KCl, 5 mM $MgCl_2$, 0−25 mM ATP, and 1 mM THP (25 °C)], its extent of phopshorylation could be monitored indirectly. Every 30 s, aliquots were quenched (15 mM EDTA) and analyzed by HPLC (method 1) to follow the formation of ADP. Extrapolation of the linear ATP hydrolysis profile to the original time of the experiment established the initial burst of ADP, equivalent to the phosphorylation stoichiometry for NAMPT.

Equilibrium Displacement by ATP. Equilibrium constants for the NAMPT-catalyzed reaction in the presence and absence of ATP were established by adding enzyme (0.6 μM) to a 6 mL reaction mixture [50 mM HEPES (pH 7.5), 50 mM NaCl, 5 mM $MgCl_2$, 1 mM THP, 100 μM PRPP, 100 μM PP_i, and 5 μM [4-^{3}H]NMN] at 25 °C. At appropriate time intervals, aliquots were quenched and analyzed by HPLC (method 1) to determine the profiles of NMN and NAM. When equilibrium was established (3 h), a small volume of ATP (leading to a final concentration of 2 mM) was added and additional aliquots were processed by HPLC after quenching. Variations in the equilibrium constant were evaluated by running two simultaneous reactions under similar conditions [0.6 μM enzyme, 50 mM HEPES (pH 7.5), 50 mM NaCl, 5 mM $MgCl_2$, 1 mM THP, 100 μM PRPP, 100 μM PP_i, and 5 μM [^{14}C]NAM], without and with ATP (2 mM).

NAMPT Kinetic Parameters without ATP. The k_{cat} and K_m of each substrate for the non-ATP-coupled NMN synthesis were determined first in the absence and then in the presence of near-saturating phosphate concentrations. To determinate the K_m for PRPP, reaction mixtures were incubated at 25 °C and contained 50−1000 μM PRPP, 1 μM [^{14}C]NAM, 50 mM HEPES (pH 7.5), 50 mM NaCl, 5 mM $MgCl_2$, and 1 mM THP. Conversion to [^{14}C]NMN was started by enzyme addition (88 nM) and monitored by quenching three samples at 5 min intervals. Separation was achieved by HPLC (method 1). The K_m for NAM was evaluated in the same way [0.5−5 μM [^{14}C]NAM, 100 μM PRPP, 50 mM HEPES (pH 7.5), 50 mM NaCl, 5 mM $MgCl_2$, 1 mM THP, and 88 nM enzyme]. Phosphate influences the initial rate and was evaluated by varying the P_i concentration from 0.25 to 5 mM using a concentrated sodium phosphate solution prebuffered at pH 7.5. A near-saturating phosphate concentration

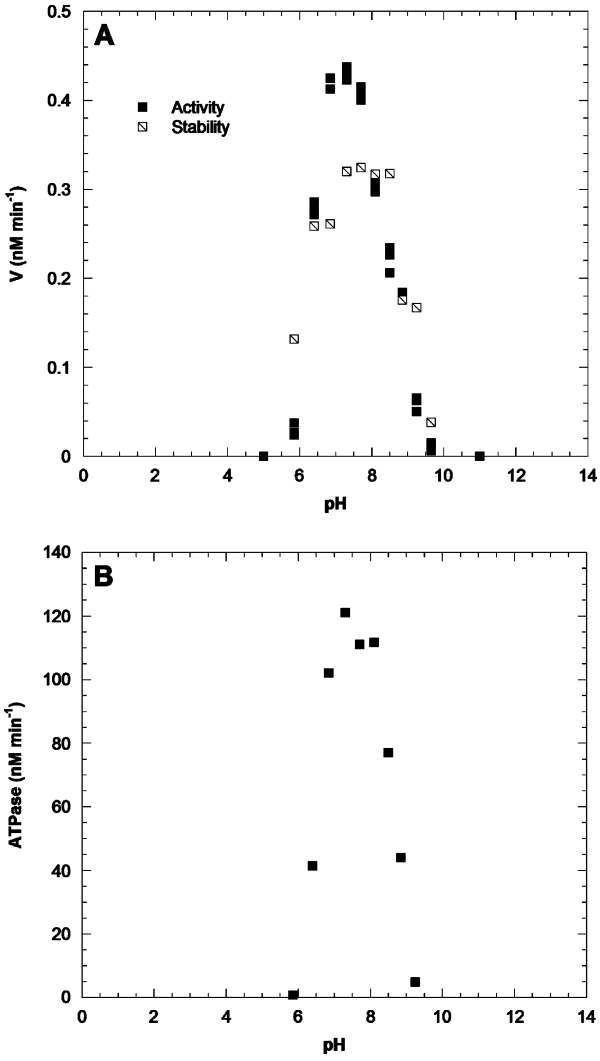

FIGURE 1: (A) NAMPT activity as a function of pH for the ATP-coupled NMN synthesis reaction. Concentrations were fixed at 1 μM [^{14}C]NAM, 200 μM PRPP, 1 mM ATP, and 5 mM $MgCl_2$ with 30 nM enzyme. (B) NAMPT ATPase activity as a function of pH. Concentrations were fixed at 2 mM ATP and 5 mM $MgCl_2$ with 0.75 μM enzyme.

was then used to determine Michaelis constants for PRPP and NAM in the presence of phosphate. The assays were the same except that each reaction mixture was supplemented with 2 mM phosphate.

NAMPT Kinetic Parameters with ATP. The k_{cat} and K_m of NAM for the ATP-coupled NMN synthesis were initially determined by a coupled fluorometric assay (*19*) slightly modified. The reactions were conducted at 25 °C, and 2.8 nM enzyme and varying concentrations of NAM (from 0.1 to 5 μM) reacted in a 3 mL sample containing 100 mM HEPES (pH 7.5), 100 mM NaCl, 10 mM $MgCl_2$, 1 mM THP, 2.5 mM ATP, 200 μM PRPP, 100 mM ethanol, 40 mM semicarbazide (to drive the ADH reaction to the formation of acetaldehyde to be trapped as its hydrazide intermediate), 80 milliunits of NMNAT-3, and 800 milliunits of ADH. NADH formation was monitored over a period of 30 min by emission of fluorescence at 455 nm upon excitation at 340 nm ($slit^{Ex}$ = 2.5 nm; $slit^{Em}$ = 12.5 nm). A second assay, the radiolabeled assay described previously, was carried out in 50 mM HEPES (pH 7.5), 50 mM NaCl, 5 mM $MgCl_2$, 1 mM THP, 2 mM ATP, 50 μM PRPP, 0.05−5 μM [^{14}C]NAM, and 1.1 nM enzyme. The corresponding K_m of NAM was obtained by extrapolation to correct for the inhibition by NAD^+. At a fixed concentration of NAD^+ of 5 μM, the ATP-coupled NMN synthesis was partially inhibited [50 mM HEPES (pH 7.5), 50 mM NaCl, 5 mM $MgCl_2$, 1 mM THP, 2 mM ATP, 50 μM PRPP, 0.05−5 μM [^{14}C]NAM, and 1.1 nM enzyme]. The corresponding Lineweaver−Burk plot led to an apparent NAM Michaelis constant (K_m^{app}). By variation of the NAD^+ concentration from 0 to 300 μM [50 mM HEPES (pH 7.5), 50 mM NaCl, 5 mM $MgCl_2$, 1 mM THP, 2 mM ATP, 50 μM PRPP, 0.1 μM [^{14}C]NAM, and 1.1 nM enzyme] and measurement of the initial rate of NMN formation at a single NAM concentration, several pairs of K_m^{app}/[NAD^+] values were obtained. Use of eq IV provides the actual K_m for NAM. The K_m values for PRPP and ATP were established for the ATP-coupled reaction with fixed substrate concentrations of 125 nM NAM, 2 mM ATP, and 0.5−500 μM PRPP and 100 nM NAM, 50 μM PRPP, and 0.4−5 mM MgATP, respectively, all at 2.2 nM enzyme.

NAMPT Inhibition. FK866, previously described as a noncompetitive inhibitor of human NAMPT (*22*), 5P-DADMe-NMN (Scheme 1), NADH, and NAD^+ were evaluated as competitive inhibitors of both non-ATP and ATP-coupled NMN synthesis, versus PRPP and NAM substrates. For the reaction involving ATP, 1 mL reaction mixtures were incubated at 25 °C and contained 200 μM PRPP, 100 nM [^{14}C]NAM, 2.5 mM ATP, appropriate inhibitor concentrations (0−80% inhibition), 5 mM $MgCl_2$, and 2.2 nM enzyme in 50 mM HEPES (pH 7.5) supplemented with 50 mM NaCl and 1 mM THP. Three samples were quenched at 15 min intervals. Corresponding initial rates, determined by HPLC (method 1), were fit as a function of the inhibitor concentration (eqs II and III). In a similar way, but with omission of ATP, K_i values for FK866 and 5P-DADMe-NMN were obtained [100 μM PRPP, 1 μM [^{14}C]NAM, 5 mM $MgCl_2$, 50 mM HEPES (pH 7.5), 50 mM NaCl, 1 mM THP, and 88 nM enzyme].

Stimulated ATPase Activity of NAMPT. The ATPase activity was evaluated under different conditions by incubating 1.5 μM enzyme and various compounds (NAM, PRPP, NMN, PP_i, and NAD^+) at 1 mM in the presence of 2 mM ATP [50 mM HEPES (pH 7.5), 50 mM KCl, 5 mM $MgCl_2$, and 1 mM THP]. Quenched samples, over 150 min, were analyzed by HPLC (method 2) to establish the steady-state rate of ADP formation.

ADP−ATP Isotope Exchange. ADP−ATP isotope exchange reactions were carried out in 50 mM HEPES (pH 7.5) with 50 mM NaCl, 5 mM free $MgCl_2$, and 1 mM THP at 25 °C. ADP (25−200 μM, containing 10^5 cpm of [2,8-^{3}H]ADP per 100 μM cold ADP) and ATP (0.2−1 mM) were present as equimolar mixtures with $MgCl_2$. The reactions were started by addition of 0.6 μM enzyme, and four samples were quenched at 15 min intervals. Nucleotides were separated by HPLC (method 1) to determine the rate of the exchange reaction. Rates of the exchange reaction were calculated as described above (eq I).

Coupling of NMN Synthesis and ATP Hydrolysis. The stoichiometry of ATP hydrolyzed per NMN formed was assayed at various ATP concentrations. The reaction mixtures (3 mL) containing 0.8−3 mM MgATP, 23 μM phosphoenolpyruvate (PEP), 23 μM NADH (with NAM at 400K_m, NAD^+, and NADH did not significantly inhibit the reaction),

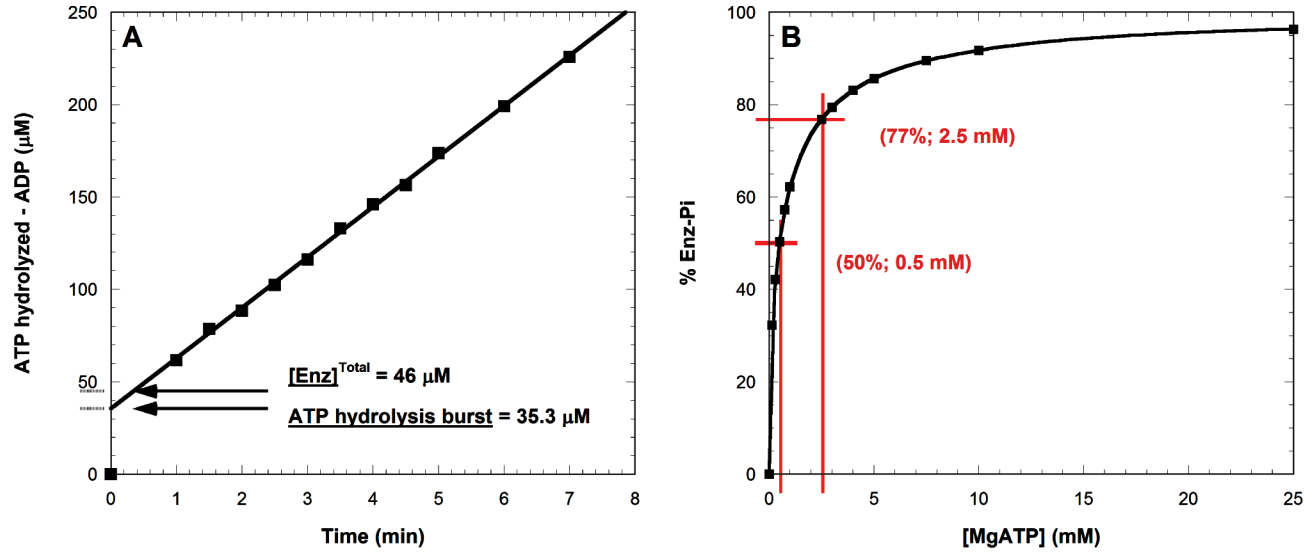

FIGURE 2: Autophopshorylation of NAMPT by ATP. Assay performed by HPLC measuring ADP formation. In panel A, NAMPT was present at 46 μM with 2.5 mM MgATP. The initial burst of ADP characterized the extent of enzyme phosphorylation. (B) Estimated fraction of NAMPT phosphorylated at various MgATP concentrations from the experiment shown in panel A.

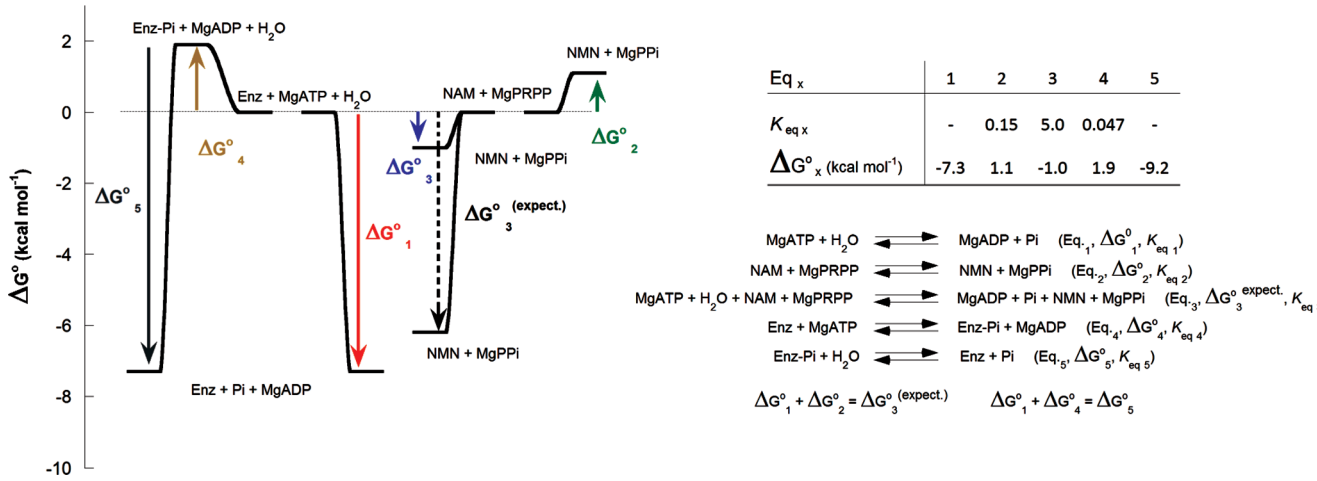

FIGURE 3: Thermodynamic model for NAMPT. Determination of K_{eq} and $\Delta G°$ for the NAMPT autophosphorylation and the non-ATP- and ATP-coupled NMN synthesis reactions at pH 7.5 (50 mM HEPES) in the presence of 100 mM KCl and 1 mM THP at 25 °C.

5 mM $MgCl_2$, 100 μM PRPP, 2 μM [^{14}C]NAM, 50 mM HEPES (pH 7.5), 50 mM NaCl, 30 mM KCl, 1 mM THP, 1 unit of PK, and 1 unit of LDH were incubated at 25 °C for 15 min (to permit trace ADP to be converted to ATP), and the reactions were started by the addition of 160 nM enzyme. The decrease in the fluorescence emission from NADH permits determination of ATP hydrolysis rates with a second-order polynomial calibration curve for fluorescence intensity from 0 to 25 μM NADH, using the following parameters: slit^{Ex} = 2.5 nm, and slit^{Em} = 2.5 nm. The same experiments were used to measure the NMN formation rates. Seven aliquots were quenched at appropriate intervals, and the amount of [^{14}C]NMN was determined by HPLC (method 1). The effect of PP_i (from 0 to 75 μM) on the ratio of ADP:NMN formation was established with a similar protocol using a fixed ATP concentration of 2.5 mM, where the ADP:NMN ratio is optimal at 1.1:1.0.

RESULTS

NAMPT Stability. NAMPT was found to be catalytically stable from pH 6.5 to 8.5 for the experimental time ranges. NMN synthesis was catalyzed with or without ATP. Optimal activity is restricted to a narrow pH range for both NMN synthesis and ATPase activities. The apparent pH optimum is 7.5, and this pH was used for the remainder of the experiments (Figure 1A).

Autophosphorylation of NAMPT. The slow steady-state ATP hydrolysis catalyzed by NAMPT was preceded by an initial burst of ADP (Figure 2A). The burst of ADP is saturable and represents the autophosphorylation of the enzyme. At 2.5 mM MgATP, 77% of NAMPT can be found phosphorylated (Figure 2B). With an estimated value of 0.047 for its K_{eq} ($\Delta G°$ = 1.9 kcal mol^{-1}), the NAMPT phopshorylation is an unfavorable reaction that leads to a high-energy species that hydrolyzes at 0.8 min^{-1} under these experimental conditions (Figure 3, eqs 4 and 5).

Effect of ATP on the Dynamic Chemical Equilibrium of NAMPT. The NAM transferase activity of NAMPT gave different equilibrium positions in the presence of ATP, consistent with coupling to the transferase reaction (Figure 4A). With addition of ATP to a preestablished equilibrium of NAMPT in a non-ATP-coupled reaction, the position of the chemical equilibrium was reversed (Figure 4B). A value

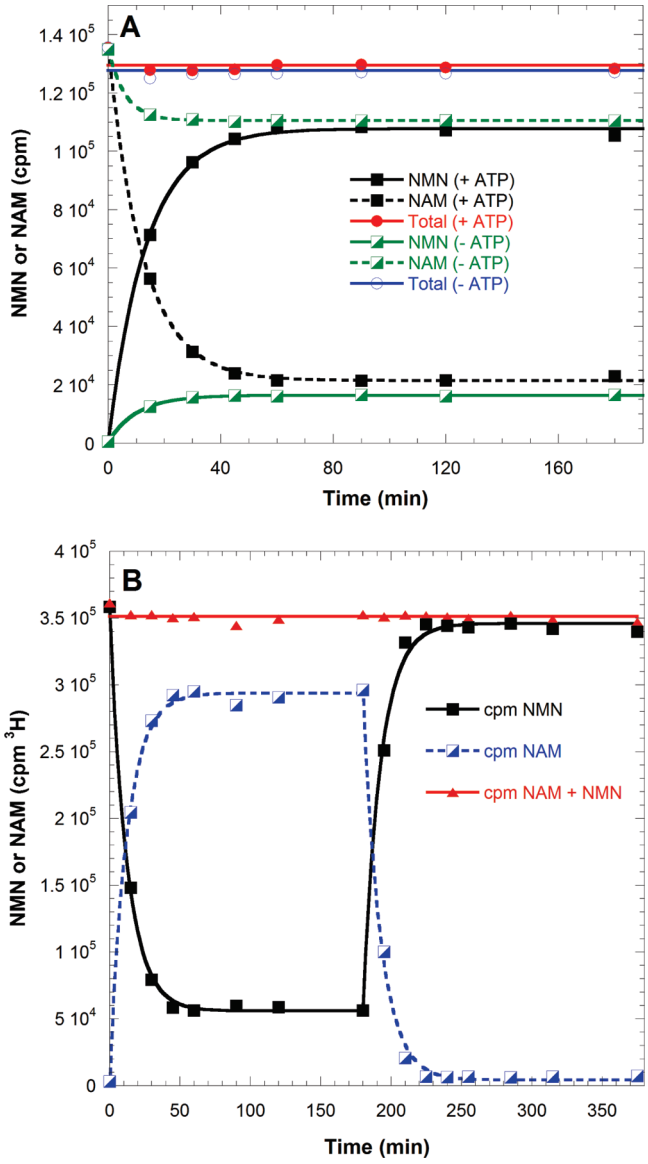

FIGURE 4: (A) Reaction equilibrium of non-ATP- and ATP-coupled NMN synthesis. NAM was originally present at 5 μM; PRPP and PP_i were present at 100 μM, and ATP was present at 2 mM. Therefore, there is no significant depletion of ATP during formation of NMN and PP_i. (B) Reversible chemical equilibrium of NAMPT as a function of ATP hydrolysis. NMN was originally present at 5 μM; PRPP and PP_i were present at 100 mM with no ATP (from 0 to 180 min). At 180 min, the concentration of the solution was made 2 mM with ATP which altered the equilibrium as shown.

Scheme 2: Continuous Fluorometric Assay for the K_m Determination of NAM (ATP-Coupled Reaction)

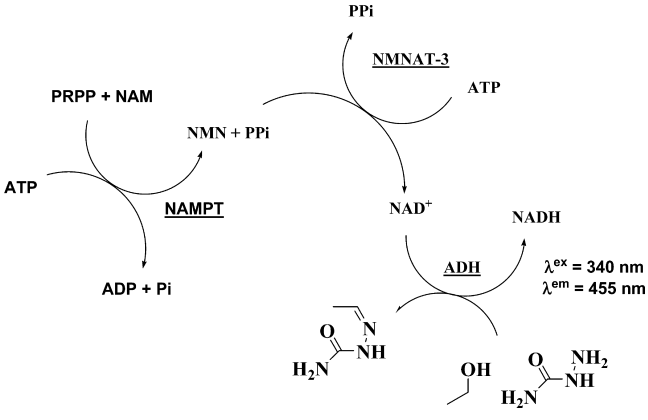

of 35 was obtained for the ratio K^{ATP}/K ($[NMN]^{ATP}[NAM]/[NMN][NAM]^{ATP}$), which is the ratio of equilibrium constants for the NAMPT reaction without including ATP, ADP, and P_i concentrations. This effect represents an energy difference of -2.1 kcal mol^{-1}, which is small compared to the energy of -7.3 kcal mol^{-1} available from ATP hydrolysis under physiological conditions, in the presence of Mg^{2+} (Figure 3, eqs 1−3). Thus, hydrolytic coupling of the ATP energy into the NAMPT reaction is weak. Nevertheless, the energy generated by ATP hydrolysis serves to thermodynamically switch the unfavorable product:substrate ratio toward production of NMN.

Effects of ATP on Kinetic Parameters. To evaluate the effects of ATP, the kinetic parameters for NAM and PRPP were determined without ATP, in the presence of P_i, and with ATP. The uncoupled reaction was studied with a radiolabeled assay, and two independent methods were used to determine the kinetic parameters of the ATP-coupled reaction. The continuous assay (Scheme 2) revealed a lower K_m value for NAM (Figure 5A) in the presence of ATP (K_m of 57 ± 6 nM with ATP compared to 855 ± 22 nM without ATP). The direct assay with [^{14}C]NAM revealed an even tighter affinity of 17 ± 2 nM for nicotinamide (Figure 5B). The inverse of the initial rate ($1/V$) as a function of reciprocal NAM concentration indicated substrate inhibition by nicotinamide concentrations as low as 250 nM. The addition of NAD^+ (5 μM) altered the kinetic properties to give linear $1/V$ versus 1/[NAM] plots. Assays with a variable concentration of NAD^+ permitted the determination of an apparent K_m (17 ± 2 nM). Even in the presence of NAD^+, nicotinamide causes substrate inhibition but with an inhibition constant near 3 μM.

Using NAD^+ as a competitive inhibitor of NMN synthesis (Figure 5C,D), several sets of $K_m^{app}/[NAD^+]$ pairs were obtained and reploted, leading to a linear relationship. This representation (eq IV), extrapolated to its ordinate intercept, allowed the determination of the actual K_m for NAM (5 ± 2 nM). This unusually small K_m value has significance for the cellular function of NAMPT in salvage of NAM for NAD^+ synthesis.

While NAMPT exhibits a high affinity for NAM, especially in the presence of ATP, the K_m for PRPP was less affected by ATP (Table 1). The K_m value for MgPRPP was 7−12 μM in the absence of ATP but was higher (K_m = 0.63 μM) in the presence of ATP.

The weak affinity between ATP and the protein is consistent with physiological conditions with cellular levels of ATP in the millimolar range. High ATP concentrations were required to saturate NAMPT (K_m = 7.4 ± 1.5 mM) and are complicated by inhibition at concentrations of >4 mM.

Despite the low rate of catalytic turnover of NAMPT, the catalytic efficiency (k_{cat}/K_m) of 1.8×10^6 M^{-1} s^{-1} is high because of the nanomolar K_m for NAM (Table 1). The ATP-coupled reaction is efficient for NAM salvage since the enzyme will catalyze formation of NMN for most collisions of a nicotinamide molecule at the active site.

Inhibition Studies. Four inhibitors [FK866, 5P-DADMe-NMN, NAD^+, and NADH (Scheme 1)] were assayed against the ATP-coupled and non-ATP-coupled reactions. In the presence of ATP, NAD^+ and NADH were competitive inhibitors versus PRPP. The relatively high affinities

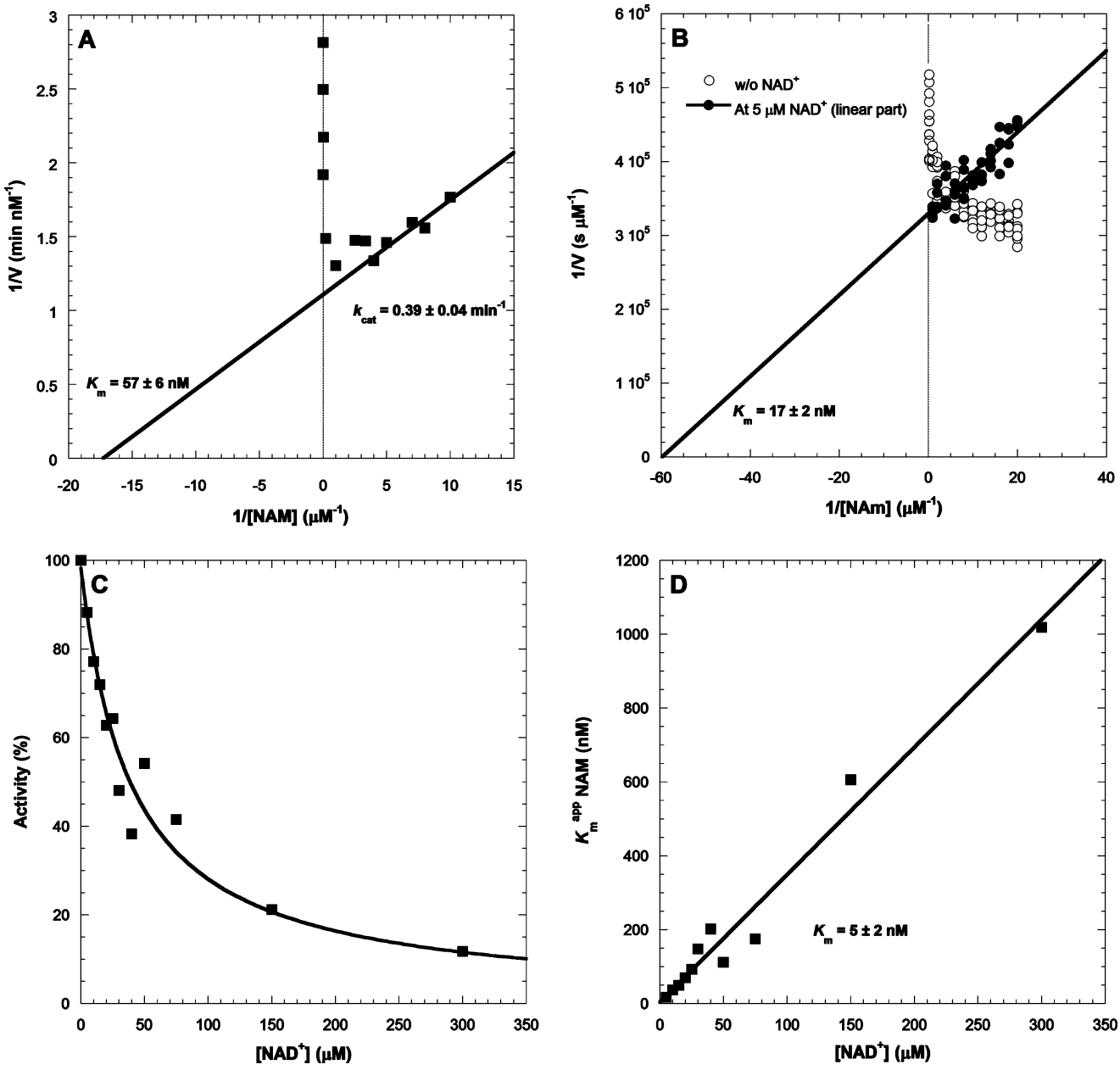

FIGURE 5: (A) Determination of kinetic parameters for NAMPT. Lineweaver−Burk representation for the K_m determination of NAM using the fluorometric coupled assay and fitting only the linear portion of the curve. (B) Lineweaver−Burk representation for the K_m determination of NAM using the direct radiolabeled assay, without and with NAD^+. (C) Profile of the NAD^+ inhibition of the ATP-coupled NMN synthesis reaction. (D) Determination of K_m for NAM for the ATP-coupled NMN synthesis. The value of the apparent K_m^{app} is plotted as a function of concentration with the value for the inhibition-free K_m value for NAM taken from the ordinate intercept to give 5 ± 2 nM.

Table 1: Kinetic Parameters of Human NAMPT for both ATP-Coupled and Non-ATP-Coupled Reactions

	non-ATP-coupled NMN synthesis		
	without P_i	with P_i	ATP-coupled NMN synthesis
K_m			
NAM (nM)	855 ± 22	235 ± 17	5 ± 2
PRPP (μM)	7.2 ± 0.6	11.7 ± 0.8	0.63 ± 0.03
ATP (P_i)[a] (mM)		0.18 ± 0.02[a]	7.4 ± 1.5
k_{cat} (min^{-1})	0.082 ± 0.001	0.085 ± 0.001	0.46 ± 0.09
k_{cat}/K_m (M^{-1} s^{-1})[b]	(1.60 ± 0.06) × 10^3	(6.1 ± 0.5) × 10^3	(1.8 ± 0.9) × 10^6

[a] K_m of P_i for the non-ATP-coupled NMN synthesis. [b] k_{cat}/K_m with respect to NAM.

of 0.14 and 0.22 μM, respectively, for these molecules are significant for the biological pathway as regulators of NAM recycling. Exhibiting a picomolar K_i, and high K_m/K_i ratios (with or without ATP), FK866 is a powerful inhibitor of NAMPT (Table 2). In contrast, 5P-DADMe-NMN (Scheme 1) was a relatively poor inhibitor of the transfer reaction (Figure 6) with K_i values of 0.5 and 7 μM with respect to PRPP and NAM, respectively. In the presence of ATP, its level of binding increased 3-fold (Table 2).

Table 2: Inhibition Results for both ATP-Coupled and Non-ATP-Coupled Reactions

	non-ATP-coupled NMN synthesis		ATP-coupled NMN synthesis[a]	
	PRPP	NAM	PRPP	NAM
K_i				
FK866 (pM)	730 ± 75 (*9863*)[b]	5000 ± 500 (*171*)	10 ± 1 (*63000*)	150 ± 18 (*33*)
5P-DADMe-NMN (μM)	0.53 ± 0.02 (*14*)	7.1 ± 0.2 (*<1*)	0.160 ± 0.015 (*4*)	2.5 ± 0.2 (*<1*)
NAD^+ (μM)		>100	0.140 ± 0.014 (*5*)	2.1 ± 0.2 (*<1*)
NADH (μM)		>100	0.22 ± 0.02 (*3*)	3.2 ± 0.2 (*<1*)

[a] K_i determined at 2.5 mM ATP. [b] Corresponding K_m/K_i ratio.

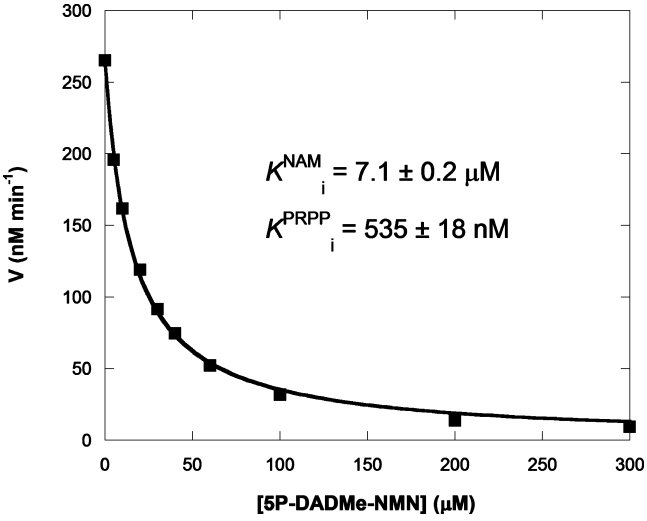

FIGURE 6: Inhibition of the non-ATP-coupled reaction by 5P-DADMe-NMN.

Stimulated ATPase Activity. ATPase activity is not tightly coupled to NMN synthesis, and the enzyme had the ability to hydrolyze ATP in the absence of other substrates (Figures 2A and 7A). Upon addition of single substrates of the transferase reaction (or mixtures of those), the ATPase function could be modulated. As described in Experimental Procedures, the free enzyme hydrolyzed the nucleotide at 0.11 min^{-1} and the rate became as slow as 0.02 min^{-1} when both substrates (forward and reverse reactions) were bound. Nicotinamide and pyrophosphate enhanced ATP hydrolysis (0.37 and 1.1 min^{-1}, respectively), while PRPP inhibited ATP hydrolysis (Figure 7A).

The PP_i-stimulated ATPase activity was further explored with the methylene and imido analogues of PP_i (PCP and PNP), assayed under the same conditions (Figure 7B). PNP had the greatest effect on ATP hydrolysis (2.6 min^{-1}), greater than the effect of pyrophosphate. However, this effect was reversible upon addition of NAM or PRPP (Figure 7C).

ADP−ATP Exchange Catalyzed by NAMPT. Phosphate is a product of the ATPase reaction of NAMPT. When the catalytic efficiencies of the enzyme in the presence of inorganic phosphate for the non-ATP-coupled NMN synthesis and the ATP-coupled reaction are compared, it is clear that P_i effects are smaller than those with ATP (Table 1). A catalytically altered His247 phosphoenzyme is proposed to exist in NAMPT. ADP−ATP isotope exchange explores conservation of a chemically exchangeable high-energy phosphate on the enzyme. ADP−ATP exchange in the absence of other reactants can occur only through the action of a high-energy phosphorylated enzyme. Figure 8A shows the results of the kinetic study for the exchange reaction. The k_{cat} for exchange was 0.9 ± 0.1 min^{-1}, and the ATP concentration required for half-maximal exchange activity was 2.2 ± 0.2 mM and the ADP concentration 0.44 ± 0.05 mM. ATP binds weakly to the phosphorylated enzyme and exhibited inhibition of NMN synthesis at concentrations higher than 4 mM.

ADP−ATP exchange occurs without NMN formation; however, the similar rates for ADP−ATP exchange (0.9 ± 0.1 min^{-1}) and NMN synthesis (0.46 ± 0.09 min^{-1}) under optimized reaction conditions suggest that formation or hydrolysis of the phosphoenzyme may be rate-limiting for the overall reaction.

ADP−ATP exchange was also carried out in the presence of 10 μM P^1,P^5-di(adenosine-5′-)pentaphosphate (Ap5A), a potent inhibitor of adenylate kinase, and the NAMPT retained the same exchange rate. Thus, adenylate kinase activity is insignificant, and the catalytic exchange site for NAMPT does not accommodate Ap5A. Another control was performed by measuring the rate of ADP−ATP exchange in the presence of 100 μM PRPP. This gave near-complete inhibition in the exchange, establishing structural or conformational linkage between these sites.

Coupling of NMN Synthesis and ATP Hydrolysis. Since only 2.1 kcal mol^{-1} of energy from the ATP hydrolysis is coupled to product formation (Figure 3), chemical stoichiometry by tight coupling can be eliminated. By comparing the rates of ATPase and NMN synthesis in the coupled transfer reaction, we found this stoichiometry (ratio R) to be ATP-dependent (Figure 8B). Only at ATP concentrations of 2.0−2.5 mM was this ratio near 1. Low concentrations of ATP result in 2 mol of ATP hydrolysis per NMN formed, and likewise, high concentrations of ATP also increased the ratio to >1. When the ATPase-transferase system was near optimal conditions (2 μM NAM, 100 μM PRPP, 2.5 mM MgATP, and 5 mM $MgCl_2$), the ratio was increased in a linear fashion with an increasing PP_i concentration (Figure 8C).

DISCUSSION

The use of ATP hydrolysis to drive enzymatic reactions requires a mechanism for coupling hydrolytic bond energy to the linked process. This distinction allows distribution of ATPases into two groups. In the first, enzymes chemically couple ATP hydrolysis by phosphorylation of a substrate-derived intermediate, and in the second, the coupling does not involve substrate phosphorylation but linked conformational changes. By similarity with bacterial NAPT (*34*), NAMPT is not catalytically dependent on the presence of ATP but has the ability to couple ATP hydrolysis and NMN synthesis. During ATP hydrolysis, NAMPT catalysis is more catalytically efficient, forward turnover is accelerated, and the unfavorable thermodynamic equilibrium for NMN for-

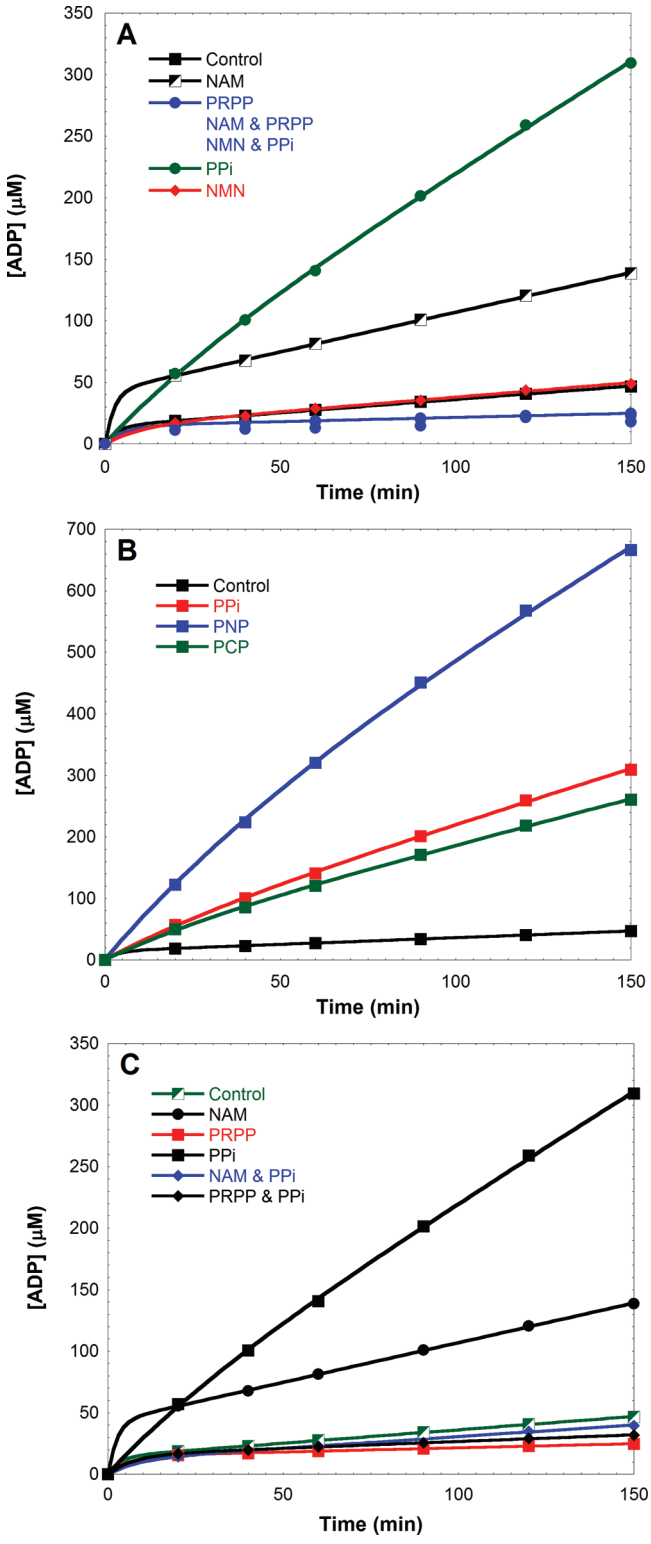

FIGURE 7: (A) NAMPT-catalyzed ATP hydrolysis and the effect of substrates and products on ATPase reaction. (B) ATPase activity of NAMPT and activation by PP_i and its analogues. (C) The presence of PRPP and/or NAM reverses the PP_i stimulation of the NAMPT ATPase reaction.

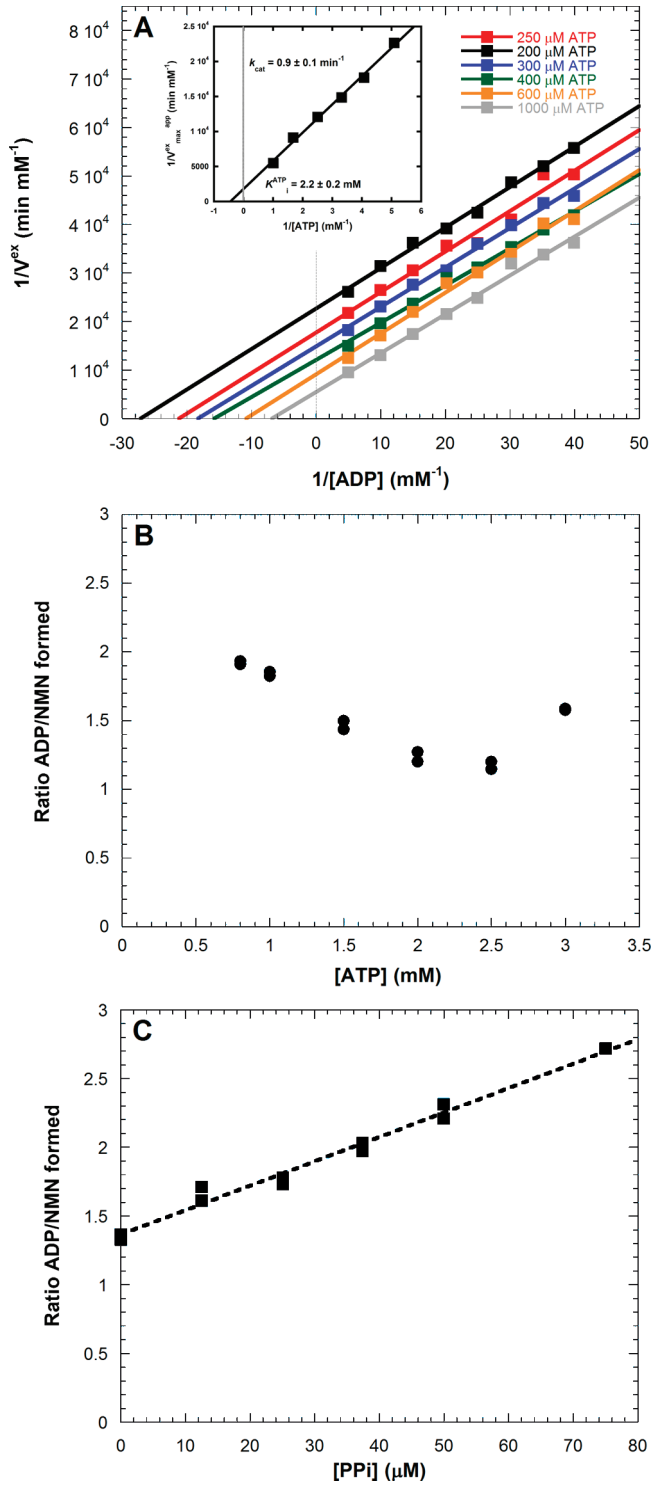

FIGURE 8: ADP−ATP isotope exchange under conditions where no NAM to NMN catalysis occurred. (A) NAMPT at a 0.6 mM concentration, with four samples quenched every 15 min. (B) Stoichiometry between ATP hydrolysis and NMN synthesis. (C) Comparison of ATP hydrolysis and NMN synthesis at increasing concentrations of PP_i.

mation is overcome. As ATP is consumed, the reaction returns to the non-ATP equilibrium position.

NAMPT uses ATP hydrolysis for thermodynamic drive, allowing the enzymatic system to build up concentrations of NMN 35-fold higher than that observed in the absence of ATP. Variations in the substrate and enzyme affinities are also influenced by ATP. The K_m value for PRPP is lowered 10-fold to a submicromolar value, ensuring adequate saturation at cellular levels of PRPP. The presence of ATP dramatically changed the interaction between NAMPT and NAM, lowering its K_m 150-fold. Moreover, with a k_{cat}/K_m value of 1.8×10^6 M^{-1} s^{-1}, the enzymatic efficiency of the ATP-coupled system is improved 1100-fold. These values are similar to those of *S. typhimurium* NAPT (*34*). The K_m values for NA (NAPT) and NAM (NAMPT) are both

Table 3: Comparison of Kinetic Parameters for Human NAMPT and *S. typhimurium* NAPT

	non-ATP-coupled NMN/NAMN synthesis		ATP-coupled NMN/NAMN synthesis	
	NAMPT	NAPT	NAMPT	NAPT
K_m				
NAM (nM)	855 ± 22	290000 ± 50000	5 ± 2	1500 ± 300
PRPP (μM)	7.2 ± 0.6	4500 ± 2200	0.63 ± 0.03	22 ± 3.3
k_{cat} (min-1)	0.082 ± 0.001	17 ± 3	$0.46 \pm 0.0.09$	174 ± 4
k_{cat}/K_m (M^{-1} s^{-1})[a]	$(1.60 \pm 0.06) \times 10^3$	$(1.0 \pm 0.4) \times 10^3$	$(1.8 \pm 0.9) \times 10^6$	$(1.9 \pm 0.6) \times 10^6$

[a] k_{cat}/K_m with respect to NAM/NA.

lowered by >100-fold, and the catalytic efficiency increased 1000−2000-fold (Table 3). However, NAMPT is unique in its unprecedented affinity for NAM, allowing the enzyme to recycle the cofactor at low nanomolar concentrations of the vitamin.

Unlike ATP, inorganic phosphate does not induce large differences in substrate affinity or catalysis. Previous studies on NAPT, the bacterial counterpart of NAMPT, demonstrated conformational modifications induced by ATP binding to the enzyme (*31, 32*) and from chemical modification (*30*) via phosphorylation of His219, the structural equivalent of His247 in human NAMPT. With NAMPT, positive ADP−ATP isotope exchange experiments establish the existence of an active phosphorylated enzyme intermediate, although attempts to isolate and characterize this species were not successful. Energetics of the NAMPT autophosphorylation describe a high-energy unstable species with a ΔG° of hydrolysis of −9.2 kcal mol^{-1}, consistent with a phosphohistidine intermediate (*36, 37*). Similarities between NAPT and NAMPT allow us to propose His247 as a candidate for the phosphorylation. This assignment is also supported by mutagenesis studies of His247 on the mouse and human enzymes (*25, 27*). The His247Glu and His247Ala mutants exhibit a decrease in substrate affinity and a lower enzymatic efficiency. Recent efforts to structurally characterize complexes of human NAMPT have provided us with X-ray data sets (*38*) containing a BeF_3^- ion in an apparent covalent interaction with His247 (manuscript in preparation).

His247 overlaps the catalytic site (*27*) and explains the competitive and substrate inhibitions seen in the kinetic data, but structural reasons for His247 phosphorylation causing NAMPT activation are not clear. Having an additional negative charge in the active site has been proposed to influence the formation of an oxacarbenium ion transition state (*27*), but this change would influence catalysis in both directions and is an unlikely explanation for forward activation. Considering the small change in k_{cat} between the ATP-coupled and uncoupled reactions (6-fold), and assuming that NMN synthesis proceeds through a single transition state, the presence of phospho-His247 would only lower the transition-state barrier by 1 kcal mol^{-1}. Such considerations suggest that other parameters involving conformational changes favorable for NAM binding are important for explaining the mechanism for ATP-coupled activation.

Hydrolysis of the phosphoenzyme is required for each catalytic turnover in NMN synthesis in the presence of ATP. The ability of exogenous PP_i to enhance ATPase indicates that hydrolysis might be triggered by this product, signaling that the reaction is complete. In stoichiometry studies with NAMPT, there is always one or more ATPs hydrolyzed per NMN formed, supporting this mechanism. It is also possible to imagine phosphoenzyme hydrolysis and rephosphorylation without full clearance of the catalytic site, consistent with more than one ATP hydrolysis event per NMN formed.

With only 2.1 kcal mol^{-1} transferred to the enzyme in the form of chemical equilibrium shifting, one could criticize the thermodynamic imperfection in this machinery. Only a few conditions result in a 1:1 stoichiometry between ATP hydrolysis and NMN formation, and slight variations of the ATP or PP_i concentration destabilized the ratio. Linkage between His247 phosphorylation and the catalytic site is demonstrated by PP_i-stimulated ATPase inhibition with either PRPP or NAM, and PRPP also inhibited the rate of ADP−ATP isotope exchange. Those observations support an overlap between the ATP−ADP binding site and those for PRPP and NAM.

Comparing the thermodynamic and kinetic aspects of NAMPT establishes that the phosphoenzyme is poised to capture NAM and PRPP, and in turn, both of these stabilize the phosphoenzyme from hydrolysis. NMN and PP_i can then be formed at concentrations that are thermodynamically prohibited without ATP coupling. The apparent energy leak in this weakly coupled reaction is transferred into a NAMPT conformation favoring the forward steps in the reaction. PP_i formation signals completion of the reaction and stimulates hydrolysis of the phosphoenzyme. The affinity of NAMPT for ATP is consistent with cellular ATP levels. Although the enzyme uses ATP energy to recycle nicotinamide, the expenditure ensures cellular NAD^+ levels with feedback regulation from NAD^+/NADH levels.

An unknown feature of phosphoribosyltransferase reactions that use ATP to shift their equilibrium is the need for ATP hydrolysis, when product PP_i hydrolysis would be more efficient in shifting the equilibrium toward products. However, coupled PP_i hydrolysis would not provide the altered kinetic properties found for NAM binding as a consequence of ATP activation.

NAMPT is essential for NMN synthesis and highly adapted to replenish the NAD^+ pool from NAM and PRPP. When NAD^+ is used in regulatory biological processes (proteins, ADP ribosylation, deacetylation), free NAM can be recycled efficiently by NAMPT using available energy in the form of ATP. Metabolic and cell developmental studies have revealed links from glucose restriction through AMP-activated protein kinase to altered transcription levels of NAMPT and altered NAD^+ levels (*39*). Finally, the inhibitions by NAD^+ and NADH are sufficiently powerful to balance NMN synthesis with needs as a function of the NAD^+/NADH pool.

ACKNOWLEDGMENT

We thank Dr. Hong Zang (Department of Biochemistry, University of Texas) for the gift of NMNAT-3 (pPROEX plasmid).

REFERENCES

1. Ziegler, M. (2000) New functions of a long-known molecule. Emerging roles of NAD in cellular signaling. *Eur. J. Biochem. 267* (6), 1550–1564.
2. Guarente, L., and Picard, F. (2005) Calorie restriction: The SIR2 connection. *Cell 120* (4), 473–482.
3. Marmorstein, R. (2004) Structure and chemistry of the Sir2 family of NAD^+-dependent histone/protein deactylases. *Biochem. Soc. Trans. 32* (6), 904–909.
4. Magni, G., Amici, A., Emanuelli, M., Orsomando, G., Raffaelli, N., and Ruggieri, S. (2004) Enzymology of NAD^+ homeostasis in man. *Cell. Mol. Life Sci. 61* (1), 19–34.
5. Araki, T., Sasaki, Y., and Milbrandt, J. (2004) Increased nuclear NAD biosynthesis and SIRT1 activation prevent axonal degeneration. *Science 305* (5686), 1010–1013.
6. Preiss, J., and Handler, P. (1958) Biosynthesis of diphosphopyridine nucleotide. I. Identification of intermediates. *J. Biol. Chem. 233* (2), 488–492.
7. D'Amours, D., Desnoyers, S., D'Silva, I., and Poirier, G. G. (1999) Poly(ADP-ribosyl)ation reactions in the regulation of nuclear functions. *Biochem. J. 342* (2), 249–268.
8. Di Lisa, F., and Ziegler, M. (2001) Pathophysiological relevance of mitochondria in NAD^+ metabolism. *FEBS Lett. 492* (1−2), 4–8.
9. Emanuelli, M., Carnevali, F., Saccucci, F., Pierella, F., Amici, A., Raffaelli, N., and Magni, G. (2001) Molecular cloning, chromosomal localization, tissue mRNA levels, bacterial expression, and enzymatic properties of human NMN adenylyltransferase. *J. Biol. Chem. 276* (1), 406–412.
10. Raffaelli, N., Sorci, L., Amici, A., Emanuelli, M., Mazzola, F., and Magni, G. (2002) Identification of a novel human nicotinamide mononucleotide adenylyltransferase. *Biochem. Biophys. Res. Commun. 297* (4), 835–840.
11. Rizzi, M., and Schindelin, H. (2002) Structural biology of enzymes involved in NAD and molybdenum cofactor biosynthesis. *Curr. Opin. Struct. Biol. 12* (6), 709–720.
12. Schweiger, M., Hennig, K., Lerner, F., Niere, M., Hirsch-Kauffmann, M., Specht, T., Weise, C., Oei, S. L., and Ziegler, M. (2001) Characterization of recombinant human nicotinamide mononucleotide adenylyl transferase (NMNAT), a nuclear enzyme essential for NAD synthesis. *FEBS Lett. 492* (1−2), 95–100.
13. Zhang, X., Kurnasov, O. V., Karthikeyan, S., Grishin, N. V., Osterman, A. L., and Zhang, H. (2003) Structural characterization of a human cytosolic NMN/NaMN adenylyltransferase and implication in human NAD biosynthesis. *J. Biol. Chem. 278* (15), 13503–13511.
14. Denu, J. M. (2003) Linking chromatin function with metabolic networks: Sir2 family of NAD^+-dependent deacetylases. *Trends Biochem. Sci. 28* (1), 41–48.
15. Hekimi, S., and Guarente, L. (2003) Genetics and the specificity of the aging process. *Science 299* (5611), 1351–1354.
16. Anderson, R. M., Bitterman, K. J., Wood, J. G., Medvedik, O., and Sinclair, D. A. (2003) Nicotinamide and PNC1 govern lifespan extension by calorie restriction in *Saccharomyces cerevisiae*. *Nature 423* (6936), 181–185.
17. Anderson, R. M., Bitterman, K. J., Wood, J. G., Medvedik, O., Cohen, H., Lin, S. S., Manchester, J. K., Gordon, J. I., and Sinclair, D. A. (2002) Manipulation of a nuclear NAD^+ salvage pathway delays aging without altering steady-state NAD^+ levels. *J. Biol. Chem. 277* (21), 18881–18890.
18. Lin, S. J., Defossez, P. A., and Guarente, L. (2000) Requirement of NAD and SIR2 for life-span extension by calorie restriction in *Saccharomyces cerevisiae*. *Science 289* (5487), 2126–2128.
19. Revollo, J. R., Grimm, A. A., and Imai, S. (2004) The NAD biosynthesis pathway mediated by nicotinamide phosphoribosyltransferase regulates Sir2 activity in mammalian cells. *J. Biol. Chem. 279* (49), 50754–50763.
20. van der Veer, E., Ho, C., O'Neil, C., Barbosa, N., Scott, R., Cregan, S. P., and Pickering, J. G. (2007) Extension of human cell lifespan by nicotinamide phosphoribosyltransferase. *J. Biol. Chem. 282* (15), 10841–10845.
21. Yang, H., Yang, T., Baur, J. A., Perez, E., Matsui, T., Carmona, J. J., Lamming, D. W., Souza-Pinto, N. C., Bohr, V. A., Rosenzweig, A., de Cabo, R., Sauve, A. A., and Sinclair, D. A. (2007) Nutrient-sensitive mitochondrial NAD^+ levels dictate cell survival. *Cell 130* (6), 1095–1107.
22. Hasmann, M., and Schemainda, I. (2003) FK866, a highly specific noncompetitive inhibitor of nicotinamide phosphoribosyltransferase, represents a novel mechanism for induction of tumor cell apoptosis. *Cancer Res. 63* (21), 7436–7442.
23. Holen, K., Saltz, L. B., Hollywood, E., Burk, K., and Hanauske, A. R. (2008) The pharmacokinetics toxicities, and biologic effects of FK866, a nicotinamide adenine dinucleotide biosynthesis inhibitor. *Invest. New Drugs 26* (1), 45–51.
24. Galli, U., Ercolano, E., Carraro, L., Blasi Roman, C. R., Sorba, G., Canonico, P. L., Genazzani, A. A., Tron, G. C., and Billington, R. A. (2008) Synthesis and Biological Evaluation of Isosteric Analogues of FK866, an Inhibitor of NAD Salvage. *ChemMedChem 3* (5), 771–779.
25. Khan, J. A., Tao, X., and Tong, L. (2006) Molecular basis for the inhibition of human NMPRTase, a novel target for anticancer agents. *Nat. Struct. Mol. Biol. 13* (7), 582–588.
26. Kim, M. K., Lee, J. H., Kim, H., Park, S. J., Kim, S. H., Kang, G. B., Lee, Y. S., Kim, J. B., Kim, K. K., Suh, S. W., and Eom, S. H. (2006) Crystal structure of visfatin/pre-B cell colony-enhancing factor 1/nicotinamide phosphoribosyltransferase, free and in complex with the anti-cancer agent FK-866. *J. Mol. Biol. 362* (1), 66–77.
27. Wang, T., Zhang, X., Bheda, P., Revollo, J. R., Imai, S., and Wolberger, C. (2006) Structure of Nampt/PBEF/visfatin, a mammalian NAD^+ biosynthetic enzyme. *Nat. Struct. Mol. Biol. 13* (7), 661–662.
28. Shin, D. H., Oganesyan, N., Jancarik, J., Yokota, H., Kim, R., and Kim, S. H. (2005) Crystal structure of a nicotinate phosphoribosyltransferase from *Thermoplasma acidophilum*. *J. Biol. Chem. 280* (18), 18326–18335.
29. Vinitsky, A., and Grubmeyer, C. (1993) A new paradigm for biochemical energy coupling. *Salmonella typhimurium* nicotinate phosphoribosyltransferase. *J. Biol. Chem. 268* (34), 26004–26010.
30. Gross, J., Rajavel, M., Segura, E., and Grubmeyer, C. (1996) Energy coupling in *Salmonella typhimurium* nicotinic acid phosphoribosyltransferase: Identification of His-219 as site of phosphorylation. *Biochemistry 35* (13), 3917–3924.
31. Rajavel, M., Gross, J., Segura, E., Moore, W. T., and Grubmeyer, C. (1996) Limited proteolysis of *Salmonella typhimurium* nicotinic acid phosphoribosyltransferase reveals ATP-linked conformational change. *Biochemistry 35* (13), 3909–3916.
32. Rajavel, M., Lalo, D., Gross, J. W., and Grubmeyer, C. (1998) Conversion of a cosubstrate to an inhibitor: Phosphorylation mutants of nicotinic acid phosphoribosyltransferase. *Biochemistry 37* (12), 4181–4188.
33. Gross, J. W., Rajavel, M., and Grubmeyer, C. (1998) Kinetic mechanism of nicotinic acid phosphoribosyltransferase: Implications for energy coupling. *Biochemistry 37* (12), 4189–4199.
34. Grubmeyer, C. T., Gross, J. W., and Rajavel, M. (1999) Energy coupling through molecular discrimination: Nicotinate phosphoribosyltransferase. *Methods Enzymol. 308*, 28–48.
35. Elliott, G. C., and Rechsteiner, M. C. (1982) Evidence for a physiologically active nicotinamide phosphoribosyltransferase in cultured human fibroblasts. *Biochem. Biophys. Res. Commun. 104* (3), 996–1002.
36. Attwood, P. V., Piggott, M. J., Zu, X. L., and Besant, P. G. (2007) Focus on phosphohistidine. *Amino Acids 32* (1), 145–156.
37. Stock, J. B., Stock, A. M., and Mottonen, J. M. (1990) Signal transduction in bacteria. *Nature 344* (6265), 395–400.
38. Data sets are deposited in the Protein Data Bank. Entry 3DKL for PRPP/benzamide/BeF_3^- complexed to NAMPT and entry 3DHF for NMN/PP_i/BeF_3^- complexed to NAMPT.
39. Fulco, M., Cen, Y., Zhao, P., Hoffman, E. P., McBurney, M. W., Sauve, A. A., and Sartorelli, V. (2008) Glucose restriction inhibits skeletal myoblast differentiation by activating SIRT1 through AMPK-mediated regulation of Nampt. *Dev. Cell 14* (5), 661–673.

BI801198M